the potential drop which occurs in the film will contribute to the photopotential. As expected, thinner, type A, GaPc-Cl films have shown much diminished photopotentials (typically less than 20 mV) for the same redox couples as in Figure 3.[3]

At illuminated GaPc-Cl/Au films, hydrogen evolution was possible at under-potentials of up to 500 mV on the as-prepared GaPc-Cl films but at very low power efficiencies (<0.001%). The shape of the SE voltammogram suggested that the photocurrents were limited by H_2-evolution kinetics rather than photon-limited, bulk conduction. Significant improvements were made when platinum catalytic sites were electrochemically deposited (less than 1 equiv of monolayer), as per the method of Heller for InP.[27] Figure 2d shows the SE voltammogram for a Pt treated GaPc-Cl electrode in a pH 1.9 buffer, compared to a Au-MPOTE electrode platinized to the same surface coverage. Hydrogen evolution occurred at 450 mV underpotential, and the slope of the $i-V$ was very close to that of the RDE studies of other redox couples. The power conversion efficiency was estimated from the i/V curves to be between 0.05 and 0.1% and is chiefly limited by the internal resistance of the Pc film. Continuous operation at an applied potential of −200 mV vs. Ag/AgCl showed a decrease of current density of 60% over 7 h. This decrease in stability could be attributed however to the loss of Pt activity—replatinizing of the electrode returned the photocurrent to the initial value. These currents were not due to trace oxygen in solution, as indicated by the lack of current observed at potentials positive of −0.40 V on the platinized-gold electrodes.

Conclusion

It is clear from these studies that the photoelectrochemical results observed with the GaPc–Cl/Au electrodes are quite encouraging for further development of organic thin films. This success and further developments hinge on the ability to grow continuous films of large, blocklike crystals of about 1 μm thickness. Previous Pc thin-film photoelectrochemical redox processes have been observed with significantly lower efficiencies which we attribute to porous films, submicrometer sized crystallites, or randomly oriented needle or platelet crystals having poor contact with the conducting substrate.[1-13] The thickness and ordering of the type C Pc films are producible at a level where the minimum defect density is ca. $10^{18}/cm^{-3}$, estimated from the Pc concentration on the edge and lattice termination sites in Figure 1 (assuming these to be the active recombination sites and ignoring possible bulk recombination sites). That defect density is within an order of magnitude of that required in the model of Rose for energy conversion using thin-film photoconductors sandwiched between two dissimilar phases.[14,15] In contrast to most single crystal materials, a higher defect density of the Pc films can be tolerated because of the smaller migration distances required of the charge carriers while still maintaining a high optical density. The efficiencies for the photoelectrochemical reactions are still considerably lower than for the single-crystal semiconductor materials.[27-30] The promise of decreasing the defect density of the ordered Pc film further and/or increasing the photoconductivity through the addition of dopants is being explored with encouraging preliminary results. The thermodynamic driving force for the photoelectrochemical processes is limited by the difference in chemical potential of an electron in the redox couple and the metal, which points to the use of metal substrates with larger work functions and aqueous couples with more extreme emf's to maximize the photovoltage of a thin-film Pc device.

Acknowledgment. This research was supported by a grant from the National Science Foundation, CHE 80-17971.

Registry No. GaPc-Cl, 19717-79-4; H_2, 1333-74-0; Pt, 7440-06-4.

(27) Heller, A.; Shalom, E. A.; Ronner, W. A.; Miller, B. *J. Am. Chem. Soc.* **1982**, *104*, 6942.

(28) Heller, A. *Acc. Chem. Res.* **1981**, *14*, 194.

(29) Rominey, R. N.; Lewis, N. W.; Bruce, J. A.; Bookbinder, D. C.; Wrighton, M. S. *J. Am. Chem. Soc.* **1982**, *104*, 467.

(30) Fan, F. F.; White, H. S.; Wheeler, B. L.; Bard, A. J. *J. Am. Chem. Soc.* **1980**, *102*, 5142.

IR Laser Induced Isomerization of $Fe(CO)_4$: A Unique Example of the Jahn–Teller Effect

Martyn Poliakoff*[1a] and Arnout Ceulemans[1b]

Contribution from the Department of Chemistry, University of Nottingham, University Park, Nottingham NG7 2RD, England, and the Department of Chemistry, University of Leuven, 3030 Heverlee, Belgium. *Received May 11, 1983*

Abstract: We present the first explanation of the non-Berry pseudorotation of $Fe(CO)_4$ (Davies, B.; McNeish, A.; Poliakoff, M.; Turner, J. J. *J. Am. Chem. Soc.* **1977**, *99*, 7573–79). A topological model, the *distortion octahedron*, is developed to represent possible distortions of a T_d four-coordinate molecule and the lowest energy isomerization pathways between equivalent C_{2v} distorted geometries. The model provides a simple rationalization of why intramolecular ligand exchange in $Fe(CO)_4$ differs from that in SF_4, which has a similar C_{2v} geometry. Our qualitative arguments are fully supported by a rigorous application of the Jahn–Teller theorem, the results of which are briefly summarized here. The precise information provided by the IR laser induced isomerization allows the distortions of $Fe(CO)_4$ to be analyzed in more detail than is usually possible with thermally induced processes.

$Fe(CO)_4$ is a coordinatively unsaturated molecule, which plays a central role in the photochemistry of $Fe(CO)_5$ and $Fe(CO)_4$-(olefin) species.[2,3] In low-temperature matrices, $Fe(CO)_4$ has been shown[4] to have a C_{2v} structure with bond angles ~145° and ~120°. The symmetry is the same as that of SF_4, but the bond angles are significantly different[5] (SF_4, 183° and 104°). $Fe(CO)_4$ has never been directly observed in solution, but recently-obtained time-resolved IR spectra show that $Fe(CO)_4$ almost certainly has

(1) (a) University of Nottingham. (b) University of Leuven.

(2) Geoffroy, G. L.; Wrighton, M. S. "Organometallic Photochemistry"; Academic Press: New York, 1979.

(3) Poliakoff, M. *Chem. Soc. Rev.* **1978**, 527–40.

(4) Poliakoff, M.; Turner, J. J. *J. Chem. Soc., Dalton Trans.* **1974**, 2276–85.

(5) Kimura, K.; Bauer, S. H. *J. Chem. Phys.* **1963**, *39*, 3172–78. Tolles, W. M.; Gwinn, W. D. *Ibid.* **1962**, *36*, 1119–21. Ewing, V. C.; Sutton, L. E. *Trans. Faraday Soc.* **1963**, *59*, 1241–7.

0002-7863/84/1506-0050$01.50/0

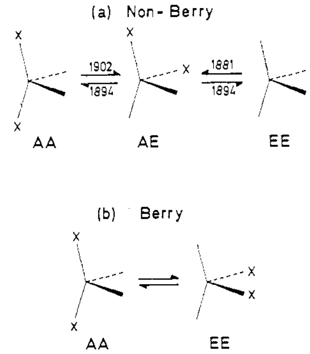

Figure 1. (a) The observed "non-Berry" pseudorotation of the isotopomers of $Fe(CO)_2(^{13}C^{18}O)_2$ in an Ar matrix and the IR frequencies (cm^{-1}) which promote interconversion.[12] X represents $^{13}C^{18}O$. (b) The Berry pseudorotation. The molecules are labeled AA, AE, and EE, where A and E refer to axial and equatorial substitution. These isotopomers were called **4**, **5**, and **6**, respectively, in ref 12. The thermal rearrangement of SF_4 is equivalent to the Berry pseudorotation.[15] Note that at the temperature of the matrix experiment, 10–30 K, all purely thermal rearrangements are frozen out and only the irradiated molecules have sufficient energy to undergo isomerization. Thus, unlike the thermal experiment the various isoenergetic interconversions (AA → AE, EE → AE, etc.) can be studied individually. The IR laser induced isomerization involves the absorption of only a single IR photon by a particular molecule, although the quantum yield is low.[12,13]

a similar C_{2v} structure in the gas phase.[6] This conclusion is supported both by approximate[7,8] and ab initio[9] molecular orbital calculations which all predict a C_{2v} structure as the minimum-energy geometry for $Fe(CO)_4$ in a *triplet ground state.* MCD spectra of matrix-isolated $Fe(CO)_4$ confirm that it is indeed paramagnetic,[10] although attempts to record the EPR spectrum have failed,[11] perhaps because of a large zero-field splitting.

Of particular relevance to this paper is the IR laser induced isomerization[12,13] of matrix-isolated $Fe(CO)_4$. When $Fe(CO)_4$ is generated from $Fe(CO)_5$ partially enriched with ^{13}CO or $^{13}C^{18}O$, one obtains a mixture of isotopomers, $Fe(^{12}CO)_{4-x}(^*CO)_x$, each of which has distinctive IR absorptions in the ν_{C-O} region. If the matrix is irradiated with a CO laser tuned to an IR frequency coincident with one of these absorptions, intramolecular ligand exchange occurs.[14] Thus, the three isotopmers of $Fe(CO)_2(^*CO)_2$ can be interconverted by IR irradiation at the appropriate frequencies, Figure 1a. This rearrangement mode of $Fe(CO)_4$ is the only known example of the non-Berry pseudorotation[12] and up till now has not been satisfactorily explained. By contrast, the ^{19}F dynamic NMR spectrum of SF_4 shows that thermal intramolecular ligand exchange in SF_4 involves a Berry pseudorotation,[15] Figure 1b, which has been rationalized by using simple

(6) Ouderkirk, A.; Wermer, P.; Schultz, N. L.; Weitz, E. *J. Am. Chem. Soc.* **1983**, *105*, 3354–5.
(7) Burdett, J. K. *J. Chem. Soc., Faraday Trans. 2* **1974**, *70*, 1599–1613.
(8) Elian, M.; Hoffman, R. *Inorg. Chem.* **1975**, *14*, 1058–76.
(9) Veillard, A. *Nouv. J. Chim.* **1981**, *5*, 599–601. Daniel, C.; Bēnard, M.; Dedieu, A.; Wiest, R.; Veillard, A., in press.
(10) Barton, T. J.; Grinter, R.; Thomson, A. J.; Davies, B.; Poliakoff, M. *J. Chem. Soc., Chem. Commun.* **1977**, 841–2.
(11) Lionel, T.; Morton, J. R.; Preston, K. F. *J. Chem. Phys.* **1982**, *76*, 234–9.
(12) Davies, B.; McNeish, A.; Poliakoff, M.; Turner, J. J. *J. Am. Chem. Soc.* **1977**, *99*, 7573–9.
(13) Poliakoff, M.; Turner, J. J. "Chemical and Biological Applications of Lasers"; Moore, C. B., Ed.; Academic Press: New York, 1981; Vol. 5, pp 175–216.
(14) P. C. Engelking and W. C. Lineberger have suggested (*J. Am. Chem. Soc.*, **1979**, *101*, 5569–73) that the isomerization could involve the dissociation of one CO group. Their suggestion was based on the low Fe–CO bond dissociation energy of $Fe(CO)_4$ deduced from their laser photoelectron spectroscopic experiments. However, this value is uncertain because of large errors in the negative ion mass spectrometric data required to calculate the bond energy, and also because the triplet ground state of $Fe(CO)_4$ made the photoelectron experiments somewhat difficult to interpret (A. E. Stevens, private communication, 1982). Our matrix experiments[12] do not support a dissociative mechanism, and in view of the uncertainties in the photoelectron results it seems unlikely.

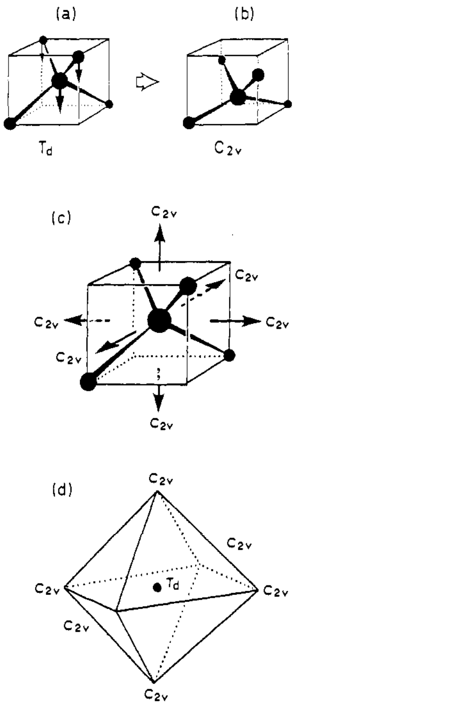

Figure 2. The geometrical derivation of the *distortion octahedron* (a) T_d $Fe(CO)_4$ inscribed in a cube. (b) The observed C_{2v} structure of $Fe(CO)_4$ inscribed in a similar cube. This structure is topologically related to T_d by the movement of the atoms in the direction of the arrows. (c) The six equivalent distortions of T_d $Fe(CO)_4$. (d) The *distortion octahedron* (explained in detail in the text) with T_d and C_{2v} points marked.

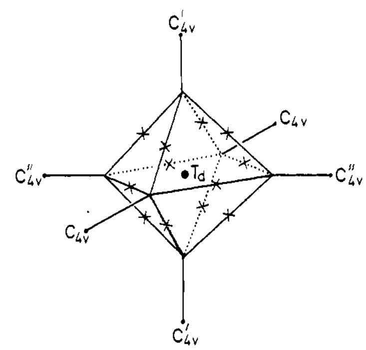

Figure 3. The *distortion octahedron* showing points representing equivalent C_s structures (centers of edges) and C_{4v} structures. Note that distortion of a T_d molecule can produce only three equivalent C_{4v} structures[21] and that each structure is represented twice on the *octahedron* as indicated by the primes.

molecular orbital arguments.[16]

In the past, topological models have been used with considerable success to enumerate isomers[17] and their interconversion pathways.[18] In this paper we derive a simple topological model, the *distortion octahedron*, to represent distortions of a tetrahedral four-coordinate molecule. We show that this model provides a simple rationalization of the non-Berry pseudorotation of $Fe(CO)_4$ and why it differs from the ligand exchange in SF_4. We indicate that the *distortion octahedron* is in reality a qualitative expression

(15) Klemperer, W. G.; Krieger, J. K.; McCreary, M. D.; Muetterties, E. L.; Traficante, D. D.; Whitesides, G. M. *J. Am. Chem. Soc.* **1975**, *97*, 7023–30.
(16) Chen, M. M. L.; Hoffmann, R. *J. Am. Chem. Soc.* **1976**, *98*, 1647–53.
(17) See, e.g.: King, R. B. *J. Am. Chem. Soc.* **1969**, *91*, 7211–15; **1970**, *92*, 6455–6459; *Inorg. Chem.* **1981**, *20*, 363–72; Rouvray, D. G. *Chem. Soc. Rev.* **1974**, *3*, 355–72.
(18) See, e.g.: Gielen, M. "Stēréochimie Dynamique"; Freund Publishing House: Tel-Aviv, 1974.

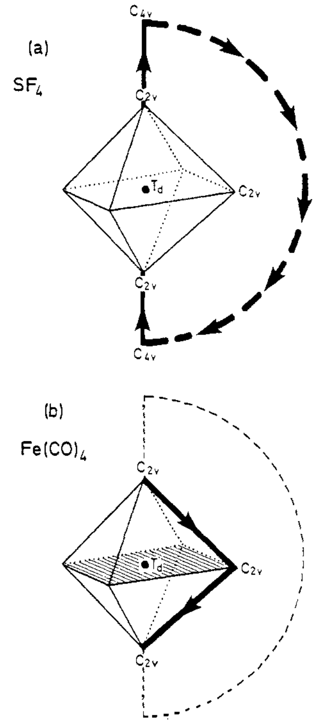

Figure 4. The lowest energy pathways for interconversion of the C_{2v} structures represtented by the top and bottom vertices of the *distortion octahedron* (a) for SF_4 and (b) for $Fe(CO)_4$—note that only one of the four equivalent pathways has been indicated for $Fe(CO)_4$.

of the Jahn–Teller theorem and that our conclusions are supported by a more rigorous Jahn–Teller analysis. Finally, we comment on the mechanism of the IR laser photochemistry of $Fe(CO)_4$ in the light of our model.

The Topological Model

(a) The "Distortion Octahedron". Imagine a T_d four-coordinate molecule inscribed in a cube, Figure 2a. This T_d structure is related *topologically* to the observed C_{2v} geometry of $Fe(CO)_4$, Figure 2b, by a movement of the Fe atom and CO groups toward one face of the cube.[19] Since all six faces of the original cube are equivalent, Figure 2a, the Fe atom (and CO groups) could have been moved toward any of the six faces to produce the observed C_{2v} geometry. Thus, there are six equivalent distortions of T_d $Fe(CO)_4$ all leading to the same C_{2v} geometry, Figure 2c. We represent these distortions using the *distortion octahedron*, Figure 2d, which is the key to our analysis of the non-Berry pseudorotation.

The center of the *octahedron* represents the undistorted T_d structure,[20] and the vertices represent the observed C_{2v} geometry. Thus, points along a line joining the center to a vertex will correspond to increasingly distorted C_{2v} structures. Similarly, all other points on the surface of the *octahedron* (and within its volume) represent particular distortions of the "parent" T_d $Fe(CO)_4$ unit. Of importance here are the C_s structures, represented by the centers of the edges, and the C_{4v} structures which are the limit of the C_{2v} distortion coordinate. (See Figure 3—note that a particular C_{4v} structure appears *twice* on the *octahedron*.[21])

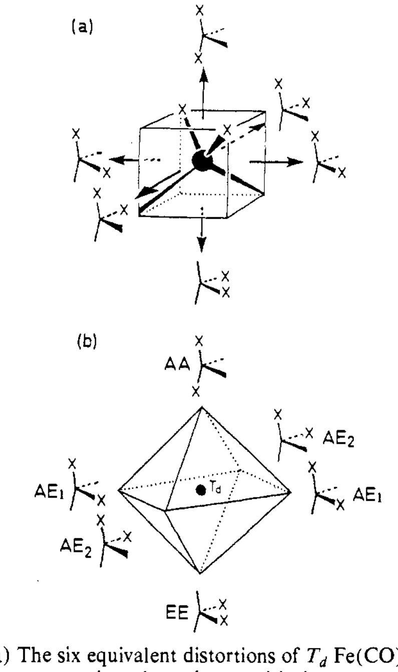

Figure 5. (a) The six equivalent distortions of T_d $Fe(CO)_2(*CO)_2$, X = *CO. All isotopomers have been drawn with the same orientation, with the C_2 axis horizontal to make identification easier. (b) The *distortion octahedron* corresponding to (a). AE_1 and AE_2 are enantiomers of isotopomer AE.

Any line on, or within, the *octahedron* represents a series of geometries along an isomerization pathway. This pathway interconverts the two structures represented by the end points of the line. Thus, an edge of the *octahedron* represents the intermediate structures on one possible $C_{2v} \rightarrow C_{2v}$ isomerization pathway.

The *octahedron* itself contains no information about the relative energies of the different distorted structures. Thus, it would be equally valid for $Fe(CO)_4$ and SF_4, although the exact meaning of the C_{2v} distortion coordinate will be different for the two molecules because the observed bond angles are different. For both SF_4 and $Fe(CO)_4$ (in a triplet ground state) the center of the *octahedron*, T_d, will be an energy maximum and the vertices will be energy minima, representing the *observed* C_{2v} geometry. For SF_4 there is a relatively low-energy C_{4v} geometry, but for $Fe(CO)_4$ any C_{4v} geometry will be of higher energy than the T_d structure. This difference arises because $SF_4(C_{4v})$ has a nonbonding[16] HOMO while $Fe(CO)_4(C_{4v})$ has an Fe–C antibonding HOMO. The result is that the lowest energy isomerization pathways for SF_4 and $Fe(CO)_4$ are different.

The low-energy pathways are shown in Figure 4. For SF_4 there is a low-energy path (via a C_{4v} geometry) connecting the C_{2v} structures represented by the top and bottom vertices of the *distortion octahedron*.[22] $C_{2v(\mathrm{top})} \rightarrow C_{4v} \rightarrow C_{2v(\mathrm{bottom})}$. This pathway is not easily accessible in $Fe(CO)_4$ because of the high energy of the C_{4v} geometry. For $Fe(CO)_4$, therefore, the lowest energy pathway connecting the top and bottom vertices must pass through a geometry represented by a point on the equatorial plane of the *octahedron* (shaded in Figure 4). Since the equatorial vertices represent energy minima (the *observed* geometry) in this plane,

(19) Our topological model is described as if the distortions of $Fe(CO)_4$ merely involved changes in bond angles without changes in bond lengths. The model would be equally valid if bond lengths did change, but this would make it more complicated to deduce the exact bond angles represented by a particular point on the *distortion octahedron*. For SF_4 the axial and equatorial bond lengths are known to be different, so a "true" C_{2v} distortion co-ordinate should involve a change in bond length.

(20) A T_d ML_4 molecule has both t_2 and e bending vibrations and so a five-dimensional diagram would be needed to represent every possible distortion. Thus, some structures are not represented on our *octahedron*, most notably D_{2d} symmetry. The T_d point of the *octahedron* would also appear on the T_d/D_{2d} distortion diagram, and so this point should be considered rigorously to represent these "missing" structures as well.

(21) Distortion of the T_d structure toward either of the opposite faces of the cube in Figure 2a will produce the same C_{4v} structure, although one structure will be inverted relative to the other. Hence the appearance of the same C_{4v} structure twice on the octahedron. In the unlikely event of all four CO groups being spectroscopically distinguishable, e.g., $Fe(^{12}CO)(^{13}CO)(C^{18}O)(^{13}C^{18}O)$, the two C_{4v} structures would be enantiomeric and no longer identical.

(22) This analysis of the isomerization of SF_4 is only qualitative since our diagram does not include all possible C_{4v} geometries or any D_{2d} geometries (see ref 20). Furthermore, the true SF_4 distortion space will be *eight* dimensional, t_2 and e bending and t_2 S–F stretching vibrational modes. Nevertheless, this pathway is consistent with that proposed in Figure 4 of ref 16. Unfortunately, an IR laser/matrix isolation experiment is not feasible with SF_4, as only one stable fluorine isotope exists.

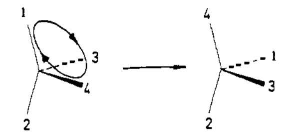

Figure 6. One possible permutation of three ligands which would explain the non-Berry pseudorotation as deduced from the *distortion octahedron.*

the lowest energy pathway must pass through these points (Figure 4).

$$C_{2v(\mathrm{top})} \rightarrow C_{2v(\mathrm{equatorial})} \rightarrow C_{2v(\mathrm{bottom})}$$

Thus, for $Fe(CO)_4$ there is no direct isomerization pathway between the top and bottom vertices, and the lowest energy pathways are topologically equivalent to the edges of the *octahedron*, i.e., via a C_s transition state.

(b) Origin of the Non-Berry Pseudorotation. In the case of $Fe(CO)_4$ and its non-Berry pseudorotation,[12] Figure 1a, the molecules have two isotopically labeled groups, i.e., $Fe(CO)_2(^*CO)_2$. Similarly, SF_4 has two sets of fluorine atoms, distinguishable by their chemical shifts.[15] This means that distortions of the T_d $Fe(CO)_2(^*CO)_2$ (or SF_4) will not produce six identical C_{2v} molecules but a mixture of the three isotopomers, AA, AE, and EE as shown in Figure 5a. These isotopomers can now be placed on the *distortion octahedron*, Figure 5b.

It is at once clear that the axially disubstituted isotopomer, AA, is at the top vertex while the equatorially disubstituted isotopomer, EE, is at the bottom. The vertices around the equator of the *octahedron* are all enantiomers of isotopomer, AE. The origin of non-Berry pseudorotation of $Fe(CO)_4$ is now apparent. There are low-energy pathways (edges of the *octahedron*) for the non-Berry pseudorotation, AA $\rightleftarrows$ AE and AE $\rightleftarrows$ EE, but no direct low-energy pathway for the Berry pseudorotation, AA $\not\rightleftarrows$ EE. The converse is true for SF_4. There are low-energy pathways between opposite vertices of the *distortion octahedron*, i.e., AA $\rightleftarrows$ EE, but none between the adjacent vertices. Thus, we see the difference between the non-Berry pseudorotation[12] of $Fe(CO)_4$ and the Berry pseudorotation[15] of SF_4.

The symmetry of the *octahedron* requires that the non-Berry pseudorotation should also interconvert the enantiomers $AE_1 \rightleftarrows AE_2$. (These are indistinguishable by IR spectroscopy and so our experiment[12] could not have detected their interconversion.) The non-Berry pseudorotation must therefore involve a "three-ligand twist" similar to that shown in Figure 6, a more complicated permutation of CO groups than originally supposed.[23]

Discussion

Our *distortion octahedron* thus provides the first simple rationalization of the non-Berry pseudorotation of $Fe(CO)_4$. It is important to stress that the geometrical derivation of the *distortion octahedron* itself involves no assumptions. Our rationalization does however rely on the statement that the lowest energy isomerization pathways of $Fe(CO)_4$ are *topologically* equivalent to the edges of the *octahedron* (i.e., only adjacent vertices are connected by low-energy pathways), and this can be more fully justified by using the Jahn–Teller theorem.

T_d $Fe(CO)_4$ is expected to be Jahn–Teller unstable with a $^3T_1$ electronic ground state which can couple to both t_2 and e vibrational modes. Although we do not explicitly invoke the Jahn–Teller theorem, our derivation of the *distortion octahedron*, Figure 2, is in effect a qualitative application of the theorem. The *octahedron* represents a three-dimensional section of the five-dimensional space of the t_2 and e C–Fe–C bending modes. In a separate publication[24] we describe a more rigorous Jahn–Teller treatment of T_d $M(CO)_4$ species, where a combination of group theory[25] and the angular overlap model[26] (AOM) is used to evaluate the relative magnitudes of the Jahn–Teller coupling constants in the general vibronic interaction Hamiltonian.[27] This approach has the advantage over the direct application of the AOM that it provides information about the general shape of the potential energy hypersurface, without having to calculate individually the energies of a large number of different distorted structures. Our Jahn–Teller calculations confirm (a) that the static distortion of T_d $Fe(CO)_4$ (to C_{2v}) should be large and (b) that the lowest energy isomerization pathway for $Fe(CO)_4$ is indeed equivalent to the edge of the *distortion octahedron*, thus validating our rationalization of the non-Berry pseudorotation.

There is nothing in our model or calculations to suggest that the IR laser induced processes are any different from thermal processes. The function of the laser is merely the selective thermal excitation of particular isotopomers. Once the energy has been absorbed by the molecule, isomerization occurs before the energy is lost to the matrix. It is this selective excitation that makes $Fe(CO)_4$ a unique example of the Jahn–Teller effect. In other molecules, either there is rapid thermal interconversion of all distorted structures or, at lower temperatures, all interchange is frozen out. In $Fe(CO)_4$, the isomerization pathways of each isotopomer can be studied individually.

Our model does not clarify the problem of how vibrational energy is transferred from the primarily C–O stretching mode, which is excited by the laser, to the C–Fe–C bending modes, which cause the isomerization. The presence of a significant Jahn–Teller effect in $Fe(CO)_4$ does, however, suggest that the density of states at 1900 cm^{-1}, due to combinations and overtones of low-frequency vibrations, may be higher than previously supposed. Thus, we cannot yet predict definitively which molecules are going to undergo IR laser induced isomerization. Nevertheless, it would seem prudent to concentrate the initial search on four-coordinate molecules, in which the Jahn–Teller coupling is anticipated to be strong,[28] e.g., $Ru(CO)_4$, $Os(CO)_4$, etc.

The *distortion octahedron* also has implications for other photochemical processes in $Fe(CO)_4$. Unfortunately, many of these are complicated by the fact that they involve a "spin-flip" as the products are diamagnetic, e.g.

$$\underset{^3B_2}{Fe(CO)_4} + CO \xrightarrow{\text{IR laser}} \underset{^1A_1'}{Fe(CO)_5}$$

Such processes are now being studied theoretically[29] and, in due course, our model can probably be extended to explain the photochemistry of matrix-isolated $Fe(CO)_4$ as comprehensively as has been done[30] for $Cr(CO)_5$.

Conclusions

The Jahn–Teller theorem has often given rise to controversy when invoked to explain experimental observations in transition-metal chemistry, because alternative rationalizations were possible. Up till now the non-Berry pseudorotation of $Fe(CO)_4$ has been a chemical oddity with no simple explanation.[31]

(23) The mechanism for the non-Berry pseudorotation, proposed in ref 13, also implies a similar twist, but this was not appreciated at the time. The twist shown in Figure 6 is not the only one that would explain the interconversion of the enantiomers. However, at least three ligands must be permuted to explain the observed isomerizations. A convenient summary of the permutations associated with pseudorotations can be found in the following Ugi, I.; Marquarding, D.; Klusacek, H.; Gillespie, P. *Acc. Chem. Res.* **1971**, *4*, 288–96.

(24) Ceulemans, A.; Beyens, D.; Vanquickenborne, L. G. *J. Am. Chem. Soc.*, submitted for publication.

(25) We have found the analysis of molecular distortions (Murray-Rust, P.; Burgi, H.-B.; Dunitz, J. D. *Acta. Crystallogr., Sect. A* **1979**, *A35*, 703–13) particularly helpful and thank Dr. R. N. Perutz for drawing our attention to it.

(26) See, e.g.: Burdett, J. K. "Molecular Shapes"; Wiley: New York, 1980.

(27) The Jahn–Teller treatment (ref 24) has been restricted to the t_2 and e bending vibrations. Since the harmonic restoring forces for metal–ligand stretches are much larger than bending force constants, it seems reasonable to suppose that coupling of the two t_2 modes will be negligible and only bending modes need be considered.

(28) Of course spin–orbit coupling may make these species behave quite differently from $Fe(CO)_4$.

(29) Veillard, A.; Dedieu, A., to be published.

(30) Burdett, J. K.; Grzybowski, J. M.; Perutz, R. N.; Poliakoff, M.; Turner, J. J.; Turner, R. F. *Inorg. Chem.* **1978**, *17*, 147–54.

(31) The very recent report (Cosandey, M.; von Büren, M.; Hansen, H.-J. *Helv. Chim. Acta* **1983**, *66*, 1–18) of a non-Berry pseudorotation in the thermal ligand exchange in (olefin) $Fe(CO)_4$ complexes is not really comparable with the case of $Fe(CO)_4$, because the symmetry of the olefin complexes is too low for a true Berry pseudorotation to occur.

However, this paper presents a rationalization which suggests that $Fe(CO)_4$ with its IR laser induced isomerization is a unique manifestation of the Jahn–Teller effect. Moreover, our topological model, the *distortion octahedron*, which was developed to study the pseudorotation, should be more generally applicable to the distortions of other four-coordinate molecules.

Acknowledgment. We thank Professors J. J. Turner and L. G. Vanquickenborne for their advice and encouragement. We thank the SERC for supporting this research and the F. Stanley Kipping Fund for a travel grant to A.C. We are grateful to Dr. M. B. Simpson and Professor J. K. Burdett for their helpful suggestions and to N. J. Bristow and Dr. G. Davidson for many discussions. A.C. thanks the Belgian National Science Foundation (NFWO) and the Belgian Government (Ministerie van het Wetenschapsbeleid) for financial support.

Registry No. $Fe(CO)_4$, 15281-98-8.

Fragments in Molecules: The Decomposition of Reaction Surfaces into Diabatic Components in the Framework of an ab Initio CI Approach

Fernando Bernardi*[1a] and Michael A. Robb*[1b]

Contribution from the Istituto Chimico G. Ciamician and Istituto di Chimica Organica, Università di Bologna, 40100 Bologna, Italy, and Department of Chemistry, Queen Elizabeth College, London W8 7AH, England. *Received January 24, 1983*

Abstract: In the present paper we describe a procedure for the computation of diabatic surfaces, defined in the framework of an ab initio CI approach. The main feature of this procedure is that each diabatic surface is associated with a specific bonding situation and thus with a specific packet of configurations built from the valence orbitals of the fragments. This computational procedure is applied here for illustrative purposes to some reactivity problems, such as the cyanate–isocyanate rearrangement, the [1,2]-sigmatropic shift in propene, a model S_N2 reaction, and the addition of singlet methylene to ethylene. It is shown that in each case this type of quantitative analysis provides a clear understanding of the origin of the various transition states occurring in these reactions.

1. Introduction

The analysis of adiabatic surfaces in terms of diabatic components is playing an increasingly important role in the interpretation of organic phenomena.[2-4] Two quantum mechanical formalisms have been essentially used for such analyses; one is related to the molecular orbital (MO) method[2,5] and the other, the LCFC (linear combination of fragment configurations) approach,[3,4] is related to the valence bond (VB) method, and both have been essentially applied at a qualitative level.

During the past 5 years there have been important technical advances in the quantum mechanical methods available for the computation of molecular potential energy surfaces, and the ab initio optimization of geometries of equilibrium and transition states is now practical.[6] We have now reached the point where it is necessary to analyze these surfaces in a quantitative way. The central problem in implementing such a computational procedure in a quantitative fashion is the formulation of a precise operational quantum mechanical definition of the diabatic surfaces themselves. In the MO method, where the orbitals are the MO's of the molecular problem under investigation, the diabatic surfaces are associated with the various MO configurations; while in the LCFC approach, where the orbitals are those of the molecular fragments or reactants, the diabatic surfaces are associated with the isolated fragment, charge transfer, and locally excited configurations. The two formalisms can be interconnected in both a qualitative and quantitative manner[7] and in the limit yield the same adiabatic surface. However, the decomposition into diabatic curves may be very different in the two models.

In the present work we shall use a LCFC formalism, with the definition that each diabatic surface describes a specific bonding situation in terms of the orbitals of the isolated fragments. This definition will lead to clearly defined diabatic surfaces and related crossings in the various kinds of reactivity problems.

In this paper we describe first a quantitative procedure based on a CI approach for computing these diabatic surfaces. All computations presented here have been performed at the STO-3G level[8] using the for the integral evaluation and the solution of the SCF equations the GAUSSIAN80 series of programs.[9] The matrix elements for the CI calculations have been computed by using the unitary group method described by Hegarty and Robb.[10]

While the quantitative procedure presented here can be applied in any atomic orbital basis, it is expected that already with a minimal basis set useful information can be obtained about the behavior of the various diabatic curves and the regions of crossings. This procedure can be used either for rationalizing the results of more sophisticated calculations or for obtaining information about

(1) (a) Università di Bologna. (b) Queen Elizabeth College. Senior CIBA-GEIGY Fellow at the University of Bologna Jan 1–August 31, 1982.
(2) "Orbital Symmetry Papers"; Simmons, H. E., Bunnett, J. F., Eds., American Chemical Society: Washington, D.C., 1974.
(3) Epiotis, N. D.; "Theory of Organic Reactions"; Springer-Verlag: Heidelberg, 1978.
(4) Epiotis, N. D. *Lect. Notes Chem.* **1982**, *29*.
(5) Woodward, R. B.; Hoffmann, R. "The Conservation of Orbital Symmetry"; Academic Press: New York, 1970.
(6) See, for example: (a) Csizmadia, I. G., Daudel, R., Eds. *NATO Adv. Study Inst. Ser., Ser. C* **1981**, *67*. (b) Whiteside, R. A.; Binkley, T. S.; Krishnan, R.; DeFrees, D. J.; Schlegel, H. B.; Pople, J. A. "Carnegie-Mellon Quantum Chemistry Archive"; Carnegie-Mellon University: Pittsburgh, 1980. (c) Schlegel, H. B. *J. Comp. Chem.* **1982**, *3*, 214–218. (d) Pulay, P. In "Modern Theoretical Chemistry"; Schaefer, H. F., III, Ed.; Plenum Press: New York, 1977; Vol. 4. (e) Osamura, Y.; Yamaguchi, Y.; Schaefer, H. F., III, *J. Chem. Phys.* **1981**, *75*, 2919–2922; **1982**, *77*, 383–390. (f) Dupuis, M. *Ibid.* **1981**, *74*, 5758–5765.
(7) (a) Shaik, S. S. *J. Am. Chem. Soc.* **1981**, *103*, 3692–3701; (b) *Ibid.* **1982**, *104*, 2708–2719; (c) *Nouv. J. Chim.* **1982**, *6*, 159–161.
(8) Hehre, W. J.; Stewart, R. F.; Pople, J. A. *J. Chem. Phys.* **1969**, *51*, 2657–2664.
(9) Binkley, J. S.; Whiteside, R. A.; Krishnan, R.; Seeger, R.; DeFrees, D. J.; Schlegel, H. B.; Topiol, S.; Kahn, L. R.; Pople, J. A. *QCPE*, **1981**, *13*, 406.
(10) Hegarty, D.; Robb, M. A. *Mol. Phys.* **1979**, *38*, 1795–1812.

0002-7863/84/1506-0054$01.50/0